

Published in final edited form as:

Gene Expr Patterns. 2014 July ; 15(2): 96–103. doi:10.1016/j.gep.2014.05.003.

A Comprehensive Analysis of Aquaporin and Secretory Related Gene Expression in Neonate and Adult Cholangiocytes

Holly M. Poling^{1,3}, Sujit K. Mohanty², Greg M. Tiao², and Stacey S. Huppert¹

Holly M. Poling: holly.poling@cchmc.org; Sujit K. Mohanty: sujit.mohanty@cchmc.org; Greg M. Tiao: greg.tiao@cchmc.org

¹Division of Gastroenterology, Hepatology, and Nutrition; Cincinnati Children's Hospital Medical Center; 3333 Burnet Avenue, Cincinnati, Ohio, 45229, United States of America

²Division of Pediatric General and Thoracic Surgery; Cincinnati Children's Hospital Medical Center; 3333 Burnet Avenue, Cincinnati, Ohio, 45229, United States of America

Abstract

Canalicular bile is secreted by hepatocytes and then passes through the intrahepatic bile ducts, comprised of cholangiocytes, to reach the extrahepatic biliary system. In addition to providing a conduit for bile to drain from the liver, cholangiocytes play an active role in modifying bile composition. Bile formation is the result of a series of highly coordinated intricate membrane-transport interactions. Proper systematic regulation of solute and water transport is critical for both digestion and the health of the liver, yet our knowledge of cholangiocyte water and ion transporters and their relative expression patterns remains incomplete. In this report, we provide a comprehensive expression profile of the aquaporin (AQP) family and three receptors/channels known to regulate ion transport in the murine cholangiocyte. In murine intrahepatic cholangiocytes, we found mRNA expression for all twelve of the members of the AQP family of proteins and found temporal changes in the expression profile occurring with age. Using AQP4, an established marker within cholangiocyte physiology, we found that AQP2, AQP5 and AQP6 expression levels to be significantly different between the neonatal and adult time points. Furthermore, there were distinct temporal expression patterns, with that of AQP12 unique in that its expression level decreased with age, whilst the majority of AQPs followed an increasing expression level trend with age. Of the three receptors/channels regulating ion transport in the murine cholangiocyte, only the cystic fibrosis transmembrane conductance regulator was found to follow a consistent trend of decreasing expression coincident with age. We have further validated

© 2014 Elsevier B.V. All rights reserved.

Corresponding Author: Stacey S. Huppert, stacey.huppert@cchmc.org, phone: 513.803.3871.

³Current location: Division of Pediatric General and Thoracic Surgery; Cincinnati Children's Hospital Medical Center; 3333 Burnet Avenue, Cincinnati, Ohio, 45229, United States of America

Disclosures: The authors have nothing to disclose.

Author Contributions

H.M.P. and S.K.M. performed the experiments. H.M.P., S.K.M., and S.S.H. designed the study and were responsible for interpretation of data. H.M.P., S.K.M., G.M.T., and S.S.H. drafted and revised the manuscript.

Publisher's Disclaimer: This is a PDF file of an unedited manuscript that has been accepted for publication. As a service to our customers we are providing this early version of the manuscript. The manuscript will undergo copyediting, typesetting, and review of the resulting proof before it is published in its final citable form. Please note that during the production process errors may be discovered which could affect the content, and all legal disclaimers that apply to the journal pertain.

AQP3 and AQP8 protein localization in both hepatocytes and cholangiocytes. This study emphasizes the need to further appreciate and consider the differences in cholangiocyte biology when treating neonatal and adult hepatobiliary diseases.

Keywords

Cholestasis; Liver; Water Transport

1 Introduction

The primary function of the exocrine liver is bile secretion; 95% of which is comprised of water [1]. Bile acts to aid in the digestion of lipids and alterations in bile composition or flow are implicated in numerous human hepatic diseases, a subset referred to as cholangiopathies. Cholangiocytes, the bile duct epithelial cells, act not only to form a conduit to facilitate the flow of bile, but also to modify bile composition [2, 3]. Given that we have no explanation, but know that an obvious difference in cholangiocyte biology exists as revealed by the window of infant susceptibility to biliary atresia in the first few months of life [4], we still have a lot to learn regarding the differences and/or similarities between neonate and adult cholangiocytes. The purpose of the present study is to describe the temporal expression pattern of the entire aquaporin (AQP) family as well as other transporters and receptors involved in regulating cholangiocyte secretion.

AQPs are a family of 12 currently described proteins that act as channels, and have been classified into three groups: 1) classical, which act to only allow the passive transport of water; 2) aquaglycerolporins, which in addition to water also facilitate the transport of small uncharged solutes, such as glycerol, ammonia and urea; and 3) unorthodox, which have been more recently discovered and whose function is not fully understood [5]. While AQP1 and AQP4 expression and localization have been well-documented in rat cholangiocytes, their presence in mouse and human cholangiocytes is less clear [6, 7]. Interestingly, mouse cholangiocytes deficient for AQP1 are not defective in water movement [8]. Understanding the AQP family transcriptional profiles will serve as a basis for future mechanistic studies of disease processes that occur at the biliary epithelial level, where altered bile flow and/or composition contribute to pathologic abnormalities [3] and potential susceptibility [9].

2 Results

2.1 Classical Aquaporin (AQP 0,1,2,4 and 5) Temporal mRNA Expression Pattern in Cholangiocytes

In conducting our gene expression analysis, we chose day of life 60 (D60) as the adult cholangiocyte endpoint. By this time point, the liver has reached a mature size and the three-dimensional biliary system is established [10]. All fold changes reported subsequently are in reference to D60 cholangiocytes. Since AQP10 is a pseudogene in mouse, its expression was not investigated [11]. AQP0, AQP1, AQP2, and AQP4 share a similar messenger RNA (mRNA) expression pattern in that fold changes increased with age before decreasing to the D60 level (Figure 1A–D). For AQP1: D2 was significantly lower than D60, while D9 and D30 were significantly higher with fold changes in the hundreds. For AQP0 and AQP2: D2

was significantly lower than D60, while D9 was indistinguishable, and D30 was significantly higher. For AQP4: D2, D9, and D30 were significantly higher than that at D60, with the largest fold change at D30. The mRNA expression pattern of AQP5 in cholangiocytes at different time points also followed an increasing trend; D2, D9 and D30 all had significantly lower expression levels than that of D60 (Figure 1E).

2.2 Aquaglyceroporin (AQPs 3, 7 and 9) Temporal mRNA Expression Pattern in Cholangiocytes

The mRNA expression pattern of AQP3 increased with age before decreasing to the D60 level. For AQP3: D2 was significantly lower than D60, while D9 and D30 were significantly higher than that at D60 (Figure 2A). The mRNA expression pattern of AQP7 was similar to AQP3 in that it increased with age, however it did not exceed that of the D60 cholangiocyte. For AQP7: D2, D9, and D30 were significantly lower than D60 (Figure 2B). The mRNA expression pattern of AQP9 did not follow a consistent trend with age. For AQP9: D2, D9, and D30 were significantly higher than D60, with a peak of expression at D9 where a fold change of almost 5000 was observed (Figure 2C).

2.3 Unorthodox Aquaporin (AQPs 8, 11 and 12) Temporal mRNA Expression Pattern in Cholangiocytes

The mRNA expression pattern of AQP6 followed an increasing trend with age. For AQP6: D2 and D9 were significantly lower than D60, while D30 was higher (Figure 3A). The mRNA expression pattern of AQP8 and AQP11 varied at early postnatal time points. For AQP8: Both D2 and D9 were significantly lower than D60, but D30 was indistinguishable from D60 (Figure 3B). For AQP11: D2 was significantly higher than D60, but D9, and D30 were indistinguishable from D60. The mRNA expression pattern of AQP12 was the only one to start out high and decrease with age (Figure 3C). For AQP12: D2, D9 and D30 were significantly higher than that at D60 (Figure 3D).

2.4 Secretory Related Gene Temporal mRNA Expression Pattern in Cholangiocytes

The mRNA expression patterns of other secretory related genes [(anion exchange protein 2 (AE2), cystic fibrosis transmembrane conductance regulator (CFTR), and secretin receptor (SR)] as described in the rat cholangiocyte model of secretin stimulated fluid secretion did not follow a common temporal expression pattern. For AE2: Both D2 and D9 were significantly lower than D60, but D30 was indistinguishable from D60 (Figure 4A). For CFTR: D2, D9, and D30 were significantly higher than D60 and follow a decreasing trend with the highest fold change occurring at D2 (Figure 4B). For SR: D2 was significantly lower than D60, while D9 was higher and D30 indistinguishable (Figure 4C).

2.5 Relative Aquaporin mRNA Expression in Adult (D60) Cholangiocytes

In rat cholangiocytes, transport of AQP1 to the apical membrane is induced by secretin while the constitutive basolateral localization of AQP4 is not influenced by secretin stimulation [12, 13]. Due to its described role in rat and mouse cholangiocyte secretion and constitutive protein localization, here, we report all fold changes in reference to D2 and D60 AQP4 [14]. This allows for 1) the observation of other AQP mRNA levels in comparison to

a well described AQP in cholangiocyte secretion and 2) may aid in indicating other key AQPs in presently undescribed models of cholangiocyte secretion. The notable changes in relativity to AQP4 from D2 to D60 cholangiocytes were AQP2, AQP5, AQP3, and AQP6. At D2, AQP2, AQP5 and AQP6 expression levels were indistinguishable from AQP4 while at D60 they were significantly higher (Figure 5). AQP3 expression was significantly lower than AQP4 at D2, while it was undistinguishable from AQP4 at D60 (Figure 5).

2.6 Aquaporin and Secretory Related Protein Expression

To verify whether proteins encoded by the transcripts we identified are detected in mouse cholangiocytes, we assessed protein localization by immunostaining liver tissue (Figure 6,7). We chose AQP1, AQP3, AQP8, and CFTR as dynamic representatives of each class of aquaporins and a secretory related protein. AQP3 and AQP8 are observed in hepatocytes as well as cholangiocytes (Figure 6). AQP1 and CFTR expression were observed in cholangiocytes, but absent from hepatocytes (Figure 6,7). Kidney tissue sections were used as a positive immunostaining control [5, 6].

3 Discussion

The results of the present study provide new information regarding the temporal AQP gene expression in wild type murine cholangiocytes with age. Most notably, we detected mRNA expression of the entire AQP family in murine cholangiocytes, which had yet to be confirmed [1, 5–7, 15–18]. Importantly, we verified protein expression of AQPs from each of the three groups (classical, AQP1; aquaglycerol, AQP3; and unorthodox, AQP8) in cholangiocytes [1, 5–7, 15–18]. Previously, AQP3 mRNA was found only in hepatocytes [19], and AQP8 mRNA in hepatocytes and cholangiocytes, but the protein expression remained to be confirmed [14]. We now demonstrate that AQP3 and AQP8 protein is localized in both hepatocytes and cholangiocytes.

Furthermore, we have detected significant changes in AQP gene expression not only of a specific AQP with age, but in relation to AQP4 at specific time points as well. This is significant in that AQP4 is the only AQP in mouse cholangiocytes to demonstrate a functional impact. Forced expression of AQP4, in cultured polarized normal mouse cholangiocytes lacking endogenous AQP4, is sufficient to increase transcellular water flow [14].

The well-described model of cholangiocyte fluid secretion is secretin induced and involves AQP1 and AQP4 in rats [5, 11, 12, 16, 17]. Our expression data in combination with previous studies demonstrating the lack of a cholestatic phenotype or changes in cholangiocyte fluid secretion in both an AQP1-null mouse and an AQP4-null mouse, suggest that other AQPs may compensate or alternative AQPs may be involved in mouse cholangiocyte fluid secretion [8, 20]. Additionally, given that rats do not have gallbladders in which the bile would be concentrated by cholangiocytes -like it is in mice and humans- there may be inherent differences in cholangiocyte biology between species. Furthermore, the production and flow of bile is drastically higher in rats than mice [21]. While a detailed characterization of rat vs. mouse cholangiocyte biology and physiology is not currently available, it is known that several surface and membrane proteins are differentially

expressed between subsets of rat and mouse cholangiocytes further supporting their functional differences [21].

At this time, mechanistic differences related to gene expression profiles and protein localization between neonate and adult cholangiocytes—in either rats, mice or humans—have not been described. However, Tanimizu et al., have described a higher degree of plasticity associated with neonatal, one-week-old, cholangiocytes compared to those from six-week-old adult mice. In culture, they demonstrate the ability of neonatal cholangiocytes to convert into functional hepatocytes whereas adult cholangiocytes are resistant to conversion. Physiologically, the *in vitro* transepithelial electrical resistance is lower in neonatal cholangiocytes when compared to those of the adult [22]. Taken together with our focused temporal expression study, a clear difference between neonatal and adult cholangiocytes can be detected in experimental settings. These studies warrant further investigation into cholangiocyte biology to better understand maturation, susceptibility, and to provide useful information for generating therapies to effectively restore physiological disruptions within cholangiocytes associated with disease.

4 Experimental Procedures

4.1 Mice

Both male and female BALB/c wild-type mice (Harlan Labs, Indianapolis, IN) were used throughout the study. They were kept in micro-isolator cages in a virus-free environment with free access to sterilized chow and water. Husbandry and experimental procedures were performed with prior approval of the Cincinnati Children's Hospital Institutional Animal Care and Use Committee. BALB/c mice were utilized for this study due to their prevalence in models of biliary atresia [23].

4.2 Neonatal Intrahepatic Cholangiocyte Isolation

Isolation of primary murine cholangiocytes at days two and nine of life were performed as previously described [24]. Briefly, livers were homogenized, digested with collagenase, and filtered before purification with a Percoll gradient (GE Healthcare Biosciences, Pittsburgh, PA). As the final step in cell population purification, cholangiocytes were incubated with an Ep-CAM antibody (Developmental Studies Hybridoma Bank, Iowa City, IA) and then Dynabeads® (Life Technologies, Grand Island, NY), allowing for a magnetic sort. Portions of each isolate were stained with the cholangiocyte marker cytokeratin 19 to verify (>90%) purity.

4.3 Adult Intrahepatic Cholangiocyte Isolation

Isolation of primary murine adult cholangiocytes at days 30 and 60 of life were performed similarly to that as previously described [25]. Briefly, a two-step collagenase perfusion of the portal vein was followed by mincing of the liver and then further collagenase digestion. The cell suspension was filtered with 90 μ m and 30 μ m meshes. A Percoll gradient, 32% atop 90%, was utilized as the final step in cell population purification. Portions of each isolate were stained with the cholangiocyte marker cytokeratin 19 to verify (>90%) purity.

4.4 Quantitative Real-Time PCR

Neonatal primary isolated cholangiocytes were cultured for expansion due to the low number of cells initially isolated before preparing RNA using TRIZOL (Invitrogen, Carlsbad, CA). Adult primary isolated cholangiocytes were immediately prepared using TRIZOL. Next, Turbo DNA-Free kit (Ambion, Austin, TX) was used to purify the RNA samples. 972 ng RNA was used for complementary DNA synthesis, performed with SuperScript II First-Strand (Invitrogen, Carlsbad, CA). Quantitative real-time reverse transcription PCR was performed using the ABI-Prism 7900 (Applied Biosystems, Foster City, CA). Aquaporin 0 (AQP0), AQP1, AQP2, AQP3, AQP4, AQP5, AQP6, AQP7, AQP8, AQP9, AQP11, AQP12, anion exchange protein 2 (AE2), cystic fibrosis transmembrane conductance regulator (CFTR), and secretin receptor (SR) messenger RNA (mRNA) was measured on pooled samples per age and ran in triplicate. All genes of interest were normalized to three housekeeping genes: glyceraldehyde-3-phosphate dehydrogenase (GAPDH), beta-actin, and hypoxanthine phosphoribosyltransferase 1 (HPRT). All data presented are normalized to GAPDH, but similar results were obtained when using beta-actin and HPRT. Primer sequences are listed in Supporting Table 1. For day two (D2) and D9 cholangiocytes, more than ten pups' isolates were pooled for analysis prior to RNA preparation. For D30 cholangiocytes, the isolates from eight mice were pooled for analysis, while the isolates of four D60 mice were pooled. For both D30 and D60 cholangiocytes, preparations were done on individual isolates and complementary DNAs were pooled prior to quantitative real-time reverse transcription PCR.

4.5 Statistical Analysis

Data was tested for normalcy and subjected to analysis of variance, Tukey's post-hoc analysis and unpaired Student t-tests when appropriate. P-values of ≤ 0.05 were considered statistically significant. In figures, significance is denoted in the following ways: * = $p < 0.05$, ** = $p < 0.01$, and *** = $p < 0.001$. Standard deviation is not reported, as the animal repeats were pooled due to experimental necessity before running in triplicate. Raw data can be found in Supporting Tables 2–7.

4.6 Immunohistochemical Analysis

Murine liver and kidney tissue was 1) fixed overnight at 4°C in 4% paraformaldehyde, processed, and embedded in paraffin or 2) incubated at 4°C in 30% sucrose and embedded in optimal cutting temperature medium. Sections were incubated overnight at 4°C for both primary and secondary antibodies in 1% bovine serum albumin in PBS. Antibodies are listed in Supporting Table 8. Bisbenzimidazole was used as a counterstain. Images were acquired using an Eclipse Ti inverted microscope system (Nikon Instruments, Inc., Tokyo, Japan) and a DS-Fi2 camera (Nikon Instruments, Inc.).

4.8 Reagents

All reagents were purchased from Sigma unless otherwise noted.

Supplementary Material

Refer to Web version on PubMed Central for supplementary material.

Acknowledgments

Financial Support

This work was supported by grants from the National Institutes of Health to G.M.T. (R01DK091566) and S.S.H. (R01DK078640).

The authors thank Dr. Markus Grompe and Dr. Mario Strazzabosco for cholangiocyte isolation protocols and guidance; Dr. Anil Menon, Dr. Simon Hogan, and Dr. Pranav-Kumar Shivakumar for primer sequences; and Bryan Donnelly, Dr. Ashley Walther, Dr. Teagan Walter, and Kari Huppert for technical assistance.

Abbreviations

AE2	Anion Exchange Protein 2
AQP	Aquaporin
CFTR	Cystic Fibrosis Transmembrane Conductance Regulator
D	Day of Life
mRNA	Messenger RNA
SR	Secretin Receptor

References

1. Lehmann GL, Larocca MC, Soria LR, Marinelli RA. Aquaporins: their role in cholestatic liver disease. *World journal of gastroenterology: WJG*. 2008; 14:7059–7067. [PubMed: 19084912]
2. Liu Y, Meyer C, Xu C, Weng H, Hellerbrand C, ten Dijke P, Dooley S. Animal models of chronic liver diseases. *American journal of physiology Gastrointestinal and liver physiology*. 2013; 304:G449–468. [PubMed: 23275613]
3. O'Hara SP, Tabibian JH, Splinter PL, LaRusso NF. The dynamic biliary epithelia: molecules, pathways, and disease. *Journal of Hepatology*. 2013; 58(3):575–582. [PubMed: 23085249]
4. Mack CL, Feldman AG, Sokol RJ. Clues to the etiology of bile duct injury in biliary atresia. *Seminars in Liver Disease*. 2012; 32(4):307–316. [PubMed: 23397531]
5. Ishibashi K, Kondo S, Hara S, Morishita Y. The evolutionary aspects of aquaporin family. *American Journal of Physiology - Regulatory, Integrative and Comparative Physiology*. 2011; 300:R566–R576.
6. Portincasa P, Calamita G. Water channel proteins in bile formation and flow in health and disease: when immiscible becomes miscible. *Molecular aspects of medicine*. 2012; 33:651–664. [PubMed: 22487565]
7. Tabibian JH, Masyuk AI, Masyuk TV, O'Hara SP, LaRusso NF. Physiology of cholangiocytes. *Comprehensive Physiology*. 2013; 3:541–565. [PubMed: 23720296]
8. Mennone A, Verkman AS, Boyer JL. Unimpaired osmotic water permeability and fluid secretion in bile duct epithelia of AQP1 null mice. *American journal of physiology Gastrointestinal and liver physiology*. 2002; 283:G739–746. [PubMed: 12181190]
9. Ampawong S, Combes V, Hunt NH, Radford J, Chan-Ling T, Pongponratn E, Grau GE. Quantification of brain edema and localization of aquaporin 4 expression in relation to susceptibility to experimental cerebral malaria. *International Journal of Clinical and Experimental Pathology*. 2011; 4(6):566–574. [PubMed: 21904632]
10. Sparks EE, Perrien DS, Huppert KA, Peterson TE, Huppert SS. Defects in hepatic Notch signaling result in disruption of the communicating intrahepatic bile duct network in mice. *Disease Models and Mechanisms*. 2011; 4(3):359–367. [PubMed: 21282722]

11. Morinaga T, Nakakoshi M, Hirao A, Imai M, Ishibashi K. Mouse aquaporin 10 gene is a pseudogene. *Biochemical and Biophysical Research Communications*. 2002; 294:630–634. [PubMed: 12056815]
12. Marinelli RA, Tietz PS, Pham LD, Rueckert L, Agre P, LaRusso NF. Secretin induces the apical insertion of aquaporin-1 water channels in rat cholangiocytes. *The American journal of physiology*. 1999; 276:G280–286. [PubMed: 9887005]
13. Marinelli RA, Pham LD, Tietz PS, LaRusso NF. Expression of aquaporin-4 water channels in rat cholangiocytes. *Hepatology (Baltimore, Md)*. 2000; 31:1313–1317.
14. Splinter PL, Masyuk AI, Marinelli RA, LaRusso NF. AQP4 transfected into mouse cholangiocytes promotes water transport in biliary epithelia. *Hepatology*. 2004; 39:109–116. [PubMed: 14752829]
15. Borgnia M, Nielsen S, Engel A, Agre P. Cellular and molecular biology of the aquaporin water channels. *Annual Review of Biochemistry*. 2000; 68:425–58.
16. Bogert PT, LaRusso NF. Cholangiocyte biology. *Current opinion in gastroenterology*. 2007; 23:299–305. [PubMed: 17414846]
17. Alleva K, Chara O, Amodeo G. Aquaporins: another piece in the osmotic puzzle. *FEBS letters*. 2012; 586:2991–2999. [PubMed: 22728434]
18. Marinelli RA, Gradilone SA, Carreras FI, Calamita G, Lehmann GL. Liver aquaporins: significance in canalicular and ductal bile formation. *Annals of hepatology*. 2004; 3:130–136. [PubMed: 15657554]
19. Ishibashi K, Sasaki S. *Japanese Journal of Clinical Medicine*. 1995; 53(1):250–257. [PubMed: 7534836]
20. Verkman AS. Physiological importance of aquaporins: lessons from knockout mice. *Current opinion in nephrology and hypertension*. 2000; 9:517–522. [PubMed: 10990371]
21. Dawson, PA.; Shneider, BL.; Hofmann, AF. *Physiology of the Gastrointestinal Tract*. 4. Academic Press; Burlington: 2006. Chapter 56 - Bile Formation and the Enterohepatic Circulation; p. 1437-1462.
22. Tanimizu N, Nakamura Y, Ichinohe N, Mizuguchi T, Hirata K, Mitaka T. Hepatic biliary epithelial cells acquire epithelial integrity but lose plasticity to differentiate into hepatocytes in vitro during development. *Journal of Cell Science*. 2013; 126(22):5239–46. [PubMed: 24046446]
23. Petersen C, Kuske M, Bruns E, Biermanns D, Wussow PV, Mildemberger H. Progress in developing animal models for biliary atresia. *European journal of pediatric surgery: official journal of Austrian Association of Pediatric Surgery ... [et al] = Zeitschrift fur Kinderchirurgie*. 1998; 8:137–141.
24. Mohanty SK, Donnelly B, Bondoc A, Jafri M, Walther A, Coots A, McNeal M, Witte D, Tiao GM. Rotavirus Replication in the Cholangiocyte Mediates the Temporal Dependence of Murine Biliary Atresia. *PLoS ONE*. 2013; 8:e69069. [PubMed: 23844248]
25. Sirica, A. Bile Duct Epithelial Cell Culture. In: Wise, C., editor. *Epithelial Cell Culture Protocols*. Humana Press; 2002. p. 37-52.

Highlights

- The mRNA of all AQP family members is expressed in isolated murine cholangiocytes.
- The temporal mRNA expression pattern of individual AQPs is dynamic.
- Neonate mRNA expression levels of AE2, CFTR, and SR are dynamic.
- AQP3 and AQP8 proteins are localized in hepatocytes and cholangiocytes.
- AQP1 and CFTR are specifically localized in cholangiocytes.

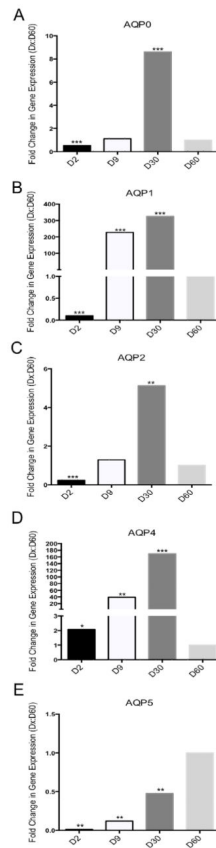


Figure 1. Relative mRNA Expression of Classical Aquaporins in Cholangiocytes
 Fold changes of classical aquaporin's mRNA levels in D2 (n > 10), D9 (n > 10), and D30 (n = 8) cholangiocytes relative to that at D60 (n = 4) assayed by RT-qPCR. Panel configuration is as follows: A) AQP0, B) AQP1, C) AQP2, D) AQP4, and E) AQP5. The level of each AQP transcript was normalized to GAPDH. Statistically significant differences, relative to D60, are indicated in the following manner: * = p< 0.05, ** = p< 0.01, and *** = p< 0.001.

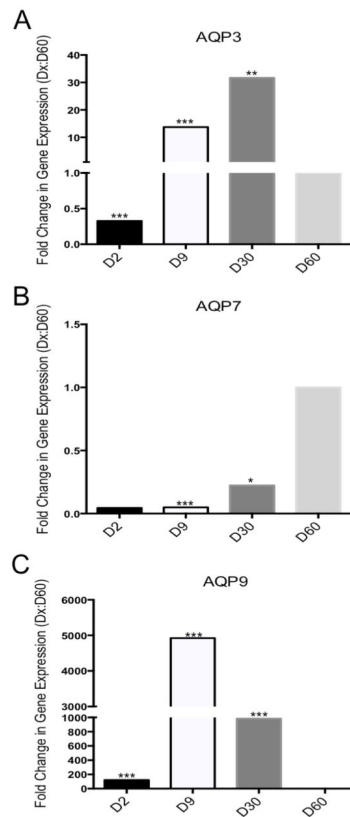


Figure 2. Relative mRNA Expression of Aquaglyceroporins in Cholangiocytes

Fold changes of aquaglyceroporin's mRNA levels in D2 (n > 10), D9 (n > 10), and D30 (n = 8) cholangiocytes relative to that at D60 (n = 4) assayed by RT-qPCR. Panel configuration is as follows: A) AQP3, B) AQP7, and C) AQP9. The level of each AQP transcript was normalized to GAPDH. Statistically significant differences, relative to D60, are indicated in the following manner: * = p < 0.05, ** = p < 0.01, and *** = p < 0.001.

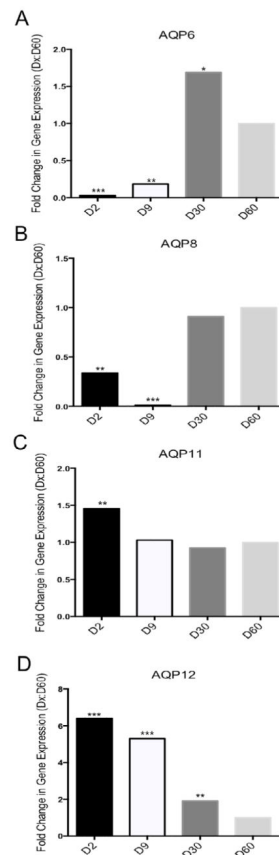


Figure 3. Relative mRNA Expression of Unorthodox Aquaporins in Cholangiocytes

Fold changes of unorthodox aquaporin's mRNA levels in D2 ($n > 10$), D9 ($n > 10$), and D30 ($n = 8$) cholangiocytes relative to that at D60 ($n = 4$) assayed by RT-qPCR. Panel configuration is as follows: A) AQP6, B) AQP8, C) AQP11, and D) AQP12. The level of each AQP transcript was normalized to GAPDH. Statistically significant differences, relative to D60, are indicated in the following manner: * = $p < 0.05$, ** = $p < 0.01$, and *** = $p < 0.001$.

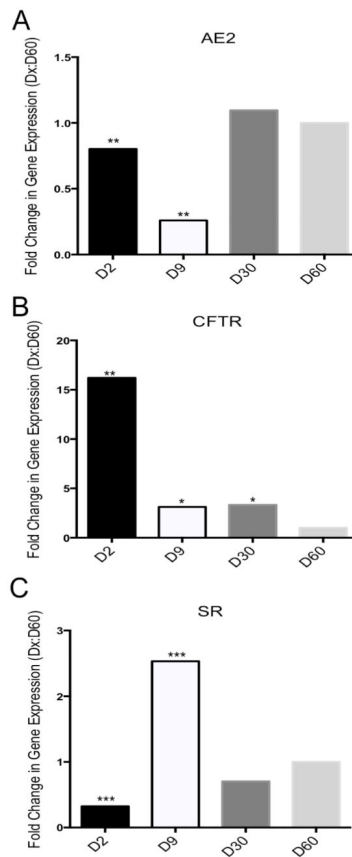


Figure 4. Relative mRNA Expression of Secretory Related Genes in Cholangiocytes

Fold changes of secretory related genes mRNA in D2 ($n > 10$), D9 ($n > 10$), and D30 ($n = 8$) cholangiocytes relative to that at D60 ($n = 4$) assayed by RT-qPCR. Panel configuration is as follows: A) AE2, B) CFTR, and C) SR. The level of each transcript was normalized to GAPDH. Statistically significant differences, relative to D60, are indicated in the following manner: * = $p < 0.05$, ** = $p < 0.01$, and *** = $p < 0.001$.

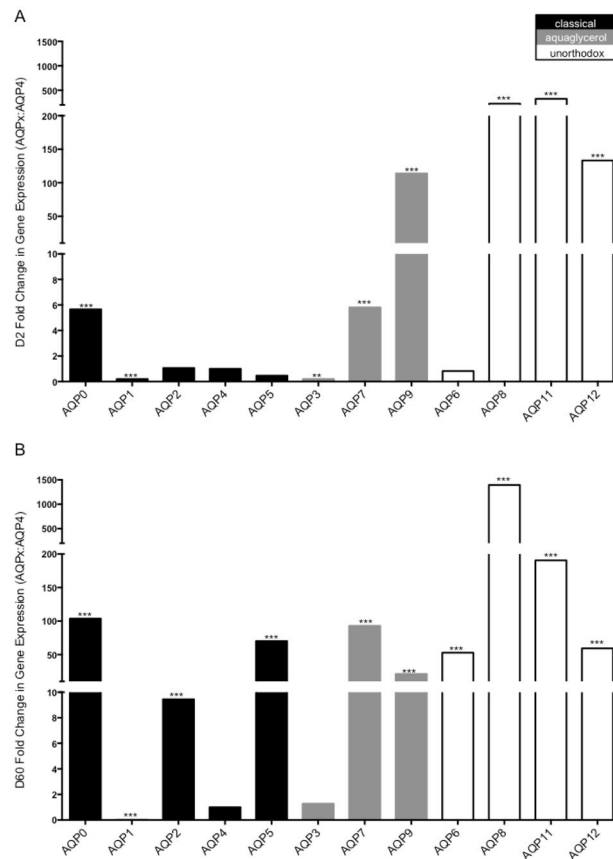


Figure 5. Relative Aquaporin mRNA Expression in Cholangiocytes at D2 and D60
 Fold changes of each aquaporin’s mRNA levels in D2 (n > 10) and D60 (n = 4) cholangiocytes relative to AQP4 assayed by RT-qPCR. Panel configuration is as follows: A) D2 and B) D60. The level of each AQP transcript was normalized to GAPDH. Statistically significant differences, relative to AQP4, are indicated in the following manner: * = p< 0.05, ** = p< 0.01, and *** = p< 0.001.

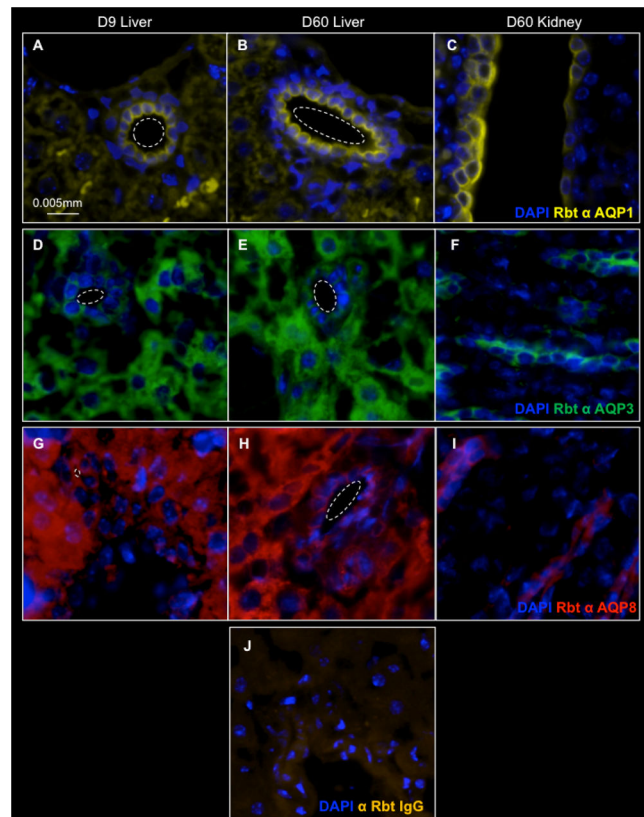


Figure 6. AQP Protein Expression in D9 and D60 Cholangiocytes

One AQP per group was examined. Dashed lines indicate the luminal space of a bile duct in liver tissue. A–C) Classical AQP1 expression in D9 Liver, D60 Liver, and D60 Kidney. D–F) Aquaglycerol AQP3 expression in D9 Liver, D60 Liver, and D60 Kidney. G–I) Unorthodox AQP8 expression in D9 Liver, D60 Liver, and D60 Kidney. J) D60 liver stained using species matched isotype control antibody.

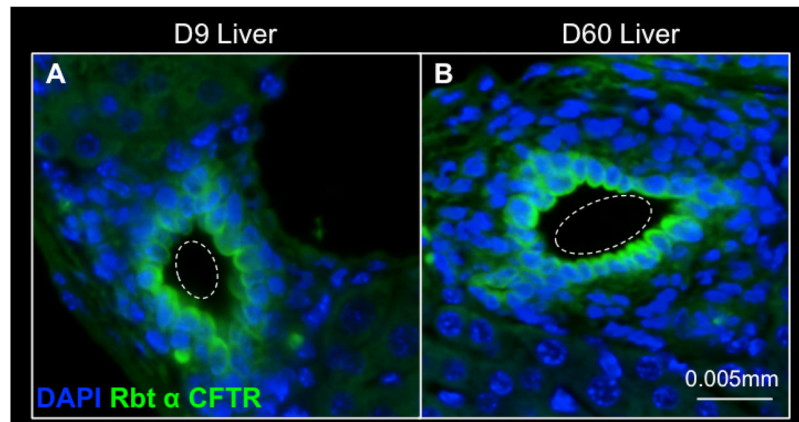


Figure 7. CFTR Protein Expression in D9 and D60 Cholangiocytes

Dashed lines indicate the luminal space of a bile duct in liver tissue. A) D9 and B) D60 cholangiocytes express the secretory related protein CFTR.